Research Article

Nano-Modified Epoxy Based Adhesive Testings: An Investigation into Apparent Shear Strength, Failure Modes, Chemical Functionals, and Microstructural Failure

Milvia O. Reis[1,2], Nathalia M. M. Paixão[1,3] , Elvis C. Monteiro[1,2] , Suchilla G. Leão[1], Hermano Nascimento Jr.[2], Antonio F. Ávila[4*]

[1]Mechanical Engineering Graduate Studies Program, Federal University of Minas Gerais, 6627 Antonio Carlos Avenue, Belo Horizonte, MG 31270-091, Brazil
[2]Stellantis Automobile Company, 3455 Contorno Avenue, Betim, MG 32669-900, Brazil
[3]Department of Mechanical Engineering, Federal Center for Technological Education of Minas Gerais, 5253 Amazonas Avenue, Belo Horizonte, MG 30421-169, Brazil
[4]Department of Mechanical Engineering, Federal University of Minas Gerais, 6627 Antonio Carlos Avenue, Belo Horizonte, MG 31270-091, Brazil
Email: avila@ufmg.br

Abstract: Single lap joints are the most used bonded joints in engineering. Unfortunately, modeling correlations between apparent shear strength and failure modes is not an easy task. This paper tries to address relationships between apparent shear strength, failure modes, and micro-structural failures. To be able to establish a correlation between chemical changes and the failure morphology of an industrial epoxy-based adhesive nano-modified by carbon nanotubes, a series of single-lap joints were prepared and tested. For this adhesive, the ductile-like fracture is controlled by changes in the aromatic ring (C-O stretching at 1,176 cm^{-1}, C-C stretching at 1,514 cm^{-1}, and C = C stretching at 1,593 cm^{-1}) and ethers group (C-O-C stretching at 1,247 cm^{-1}). Changes in the ethers group, however, have less influence than the ones in aromatic rings. Variations in oxirane groups (C-O-C stretching at 836 cm^{-1}, and rotations of CH$_2$ at 695 and 756 cm^{-1}) are more related to brittle-like microscopic failure. A small number of chemical bonds, specifically characterized by low chemical functional intensity, are associated with premature or brittle-like failure. However, concurrently, another mechanism that existed simultaneously was the ability of carbon nanotubes to alter the path of propagating cracks. This phenomenon was experimentally spotted. The macroscopic cohesive failure is controlled by the ductile-like failure at microscopic failure, while the adhesive failure is related to the brittle-like failure. Moreover, for the first time two different conditions, i.e., macroscopic quantities, apparent shear strength, failure modes, and microscopic quantities of brittle/ductile areas aspect ratios are combined in a mathematical model. This model can predict single-lap joint failure strength based on microscopic quantities.

Keywords: epoxy adhesives, chemical functional, failure modes, carbon nanotubes

1. Introduction

The automotive industry is always in pursuit of achieving lightweight and high-strength structures [1]. The idea

of weight reduction is directly linked to energy efficiency. The European Union (EU) regulations are seeking not only energy efficiency but also CO_2 reduction [2]. Tajudeen et al. [3] pointed out that the automotive industry is responsible for a significant amount of CO_2 generated around urban areas. The CO_2 reduction is based on two scenarios, i.e., environment and a social-economical component [4]. As the automotive industry hires a large number of employees, it is imperative to reduce its carbon footprint as a way of fulfilling the new environmental regulations. One possible solution for mitigating the automotive industry's carbon footprint is the usage of bonded joints. Bonded joints are less energy intensive than welding and it does not cause stress concentration problems as in bolted joints [5]. Therefore, bonded joints have a large potential for carbon footprint reduction and at the same time provide a venue for an efficient manufacturing process, especially in the automotive industry.

To be able to improve the performance's bonded joints, different strategies were tested, e.g., new designs [6], [7], different approaches [8]-[10] and nanostructures addition to adhesives/polymeric matrices [11], [12]. The potential benefits of different nanostructures in addition to different polymetric matrices/adhesives are well established in the literature [13], [14]. Some benefits are the porosity reduction [15], [16], and the increase of epoxy-based adhesives bearing loads [6]. The addition of CNTs to epoxy systems can also improve mechanical properties, i.e., tensile strength, Young's modulus, and fracture toughness [17]. Monteiro and Avila [18] credited the load-bearing enhancement to the homogeneous distribution of carbon nanotubes around the adhesive/adherent interface. Oliva and Avila [19] even reported an increase in load bearing by around 116% for a 2.0 wt% of CNT in addition to epoxy-based adhesives. Another carbon-based nanostructure, i.e., graphene, was also studied as a strategy to improve adhesives' mechanical properties. The multi-layered graphene addition to epoxy systems promotes an increase in mechanical properties and at the same time physical chemical changes [20]. The results reported by Leão et al. [20] are consistent with the ones described by Avila et al. [21] for nanoclay/epoxy systems, where vibration modes were affected by the nanoclay addition. A later study performed by Duarte et al. [22] identified different vibration behaviors based on the amount of nanoclay dispersed and its spatial distribution. The nanoparticles' dispersion into epoxy systems can easily be performed using a high-shear mixer with temperature control. By applying this strategy, Santiago et al. [23] not only got exfoliated nanostructures but also observed significant mechanical properties improvements for static and dynamic conditions. The distinct dynamic behavior of nanoclay/epoxy systems was detected by Avila et al. [24]. Avila et al. [25] experientially detected an increase in energy dissipation during low velocity by a factor of two.

Unfortunately, none of these authors addressed how the Carbon Nanotubes (CNT), graphene, or nanoclay addition changes the epoxy's chemical functionals and how failure modes were affected by these changes. This paper investigates the effects of the addition of Carbon Nanotubes (CNT) to an industrial epoxy-based monocomponent adhesive, usually employed in the automotive industry, based on chemical functionals and failure analysis, and apparent shear strength. Likewise, for the first time two different conditions, i.e., macroscopic quantities, apparent shear strength, failure modes, and microscopic quantities of brittle/ductile areas aspect ratios are combined in a mathematical model.

2. Materials and experimental methods

The nano-adhesive employed in this research is a combination of a monocomponent epoxy system, diglycidyl bisphenol A - SikaPower-456LB® commonly used in the automotive industry, and carbon nanotubes [26]. SikaPower-456LB is a viscous monocomponent epoxy system, i.e., 63,000 mPa·s, specific density of 1.3-1.5 g/cm^3, and minimum shear strength of 10 MPa [26]. The adherent used in the single-lap joint is a hot-dip galvanized low-carbon steel (yield stress 182 MPa, ultimate stress 294 MPa) with a thickness of 0.8 mm and a zinc coating of 7.5 μm supplied by USIMINAS Steel [27]. Different from Ejaz et al. [28], where adherent surface treatment was suggested, to be able to simulate the industrial environment, no surface treatment was used. The surface cleaning was performed using acetone only. As for the single-lap joint dimensions, this research follows ASTM standard D 1002, for detailed information see Figure 1 [29]. The lap joint correct alignment was guaranteed by using an in-house device developed by Nascimento Jr et al. [27]. Figure 2(a) shows the device opened, while Figure 2(b) displays the single-lap joints with the adhesive. The adhesive thickness obtained using such a device was 0.2 mm.

The dispersion of nanostructures, i.e., carbon nanotubes and graphene are dependent on different factors. For solutions with a viscosity of up to 40,000 mPa·s, e.g., Araldite 2011, the methodology proposed by Ejaz et al.

[30] is adequate. However, when the viscosity is even higher, i.e., 63,000 MPa·s (SikaPower 465), an alternative solution must be employed. Based on the design of the experiment matrix, the multi-walled carbon nanotubes, at different concentrations (0.0 wt%, 0.25 wt%, 0.50 wt%, and 1.0 wt%), were dispersed in the epoxy adhesive using the methodology proposed by Nascimento Jr et al. [27]. At least six samples were tested for each group. The CNTs' exfoliation process was guaranteed by a series of experiments conducted by dos Reis et al. [26], [31], including SEM observations. The cure cycle employed can be described by three phases, i.e., heating process: from 25 °C to 160 °C at 1 °C/min; stability process: 20 minutes at 160 °C; cooling process: from 160 °C to 25 °C at 1 °C/min. The morphological analysis was done using a Philips XL Scanning Electron Microscope (SEM) at 20.0 KV. The Fourier-Transform Infrared (FTIR) Spectroscopy procedure follows the methodology proposed by Reis et al. [26]. Table 1 summarizes the design of the experiment matrix.
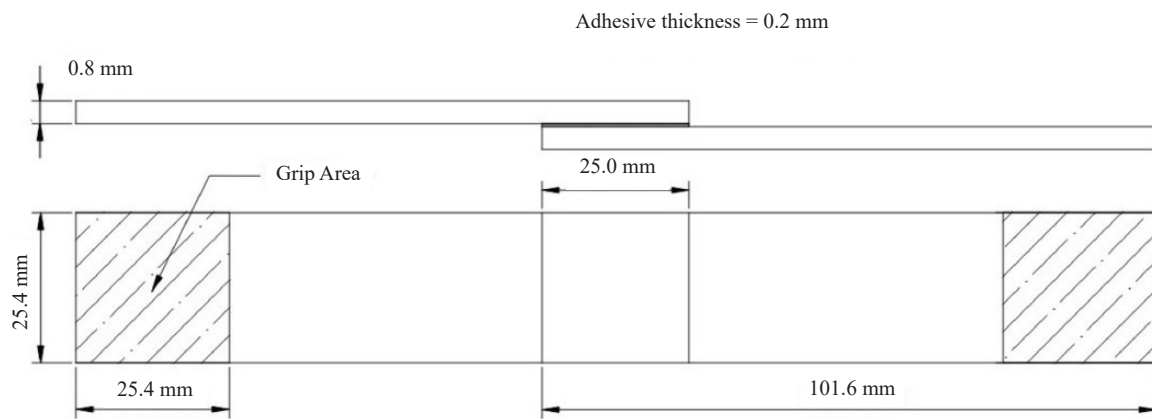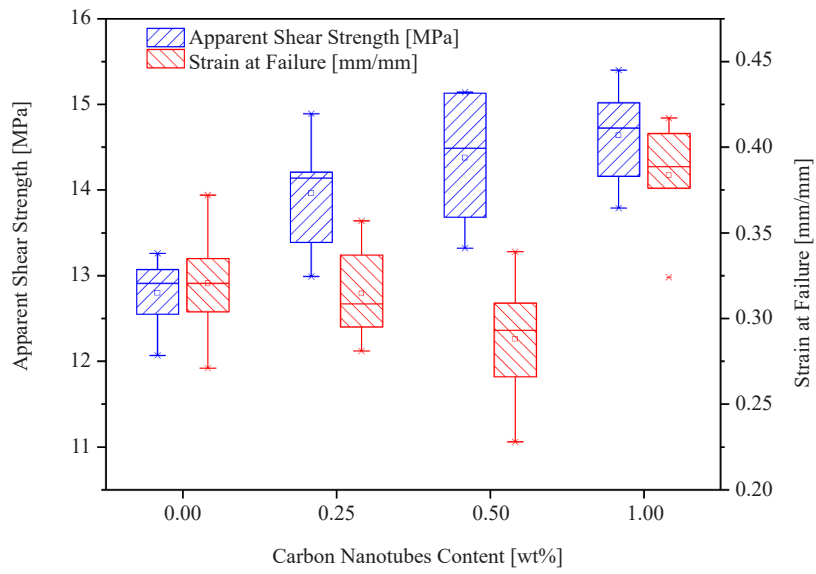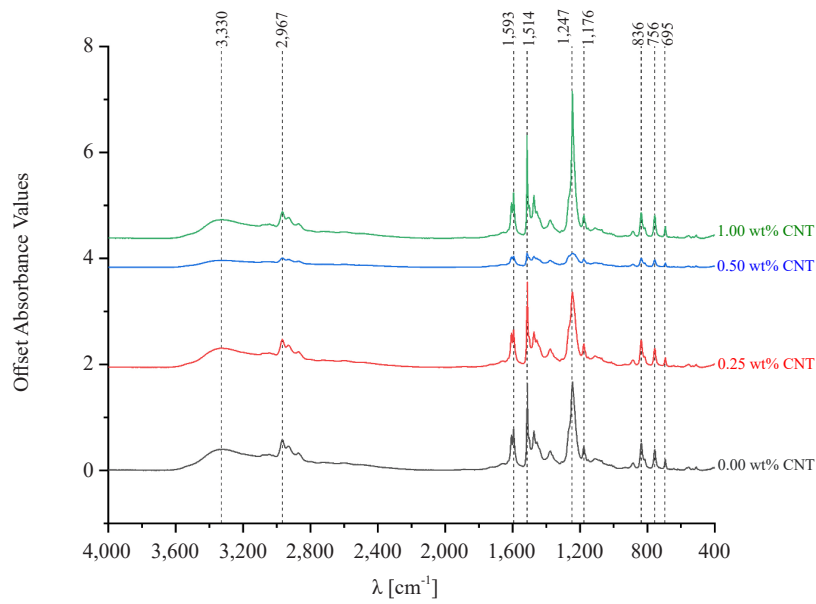

Figure 1. Single-lap joint dimensions

(a)

(b)

Figure 2. In-house device for single-lap joint preparation

Table 1. Design of experiment matrix representation

| Group ID	Epoxy [wt%]	CNT [wt%]
P-0.00	100.00	0.00
P-0.25	99.75	0.25
P-0.50	99.50	0.50
P-1.00	99.00	1.00

(a)

(b)

Figure 3. Nano-adhesive experimental data: (a) Mechanical properties; (b) FTIR signatures

3. Results and discussion

Figure 3(a) shows the apparent shear strength and strain at the failure box plot for the baseline samples (P-0.00) and the three groups with the CNT addition. The CNT addition improved the adhesive's apparent shear strength by roughly 14.2%, while the strain at failure had an increase of around 19.2%. However, the ANOVA analysis indicates no statistical difference among the three groups with CNT addition (P-0.25, P-0.50, and P-1.00). When the morphological analysis is performed a different scenario is observed. Still, before performing the morphology analysis some points must be clarified. As discussed by Zeng and Sun [32], the peak stresses, i.e., peel and shear, inside the adhesive bonded line of a single-lap joint are around the overlap edge region. This is due to the singularity condition encountered in this region. The failure initiates at this singularity region. Therefore, the morphological failure analysis focuses on this region. Moreover, to be able to have a micrograph representative of the morphological failures, a previous screening of all samples' morphological failures was performed. Figures 4(a-d) are typical morphologies of all four groups investigated. Before analyzing the fracture micrographs, it is important to define two different types of morphologies, i.e., brittle-like and ductile-like. As discussed by Naderi and Ebrahimi [33], brittle-like morphologies can be defined as large cleavage and smooth formations. According to Korayem et al. [34], a ductile-like fracture can be defined as an agglomeration of small fractures.
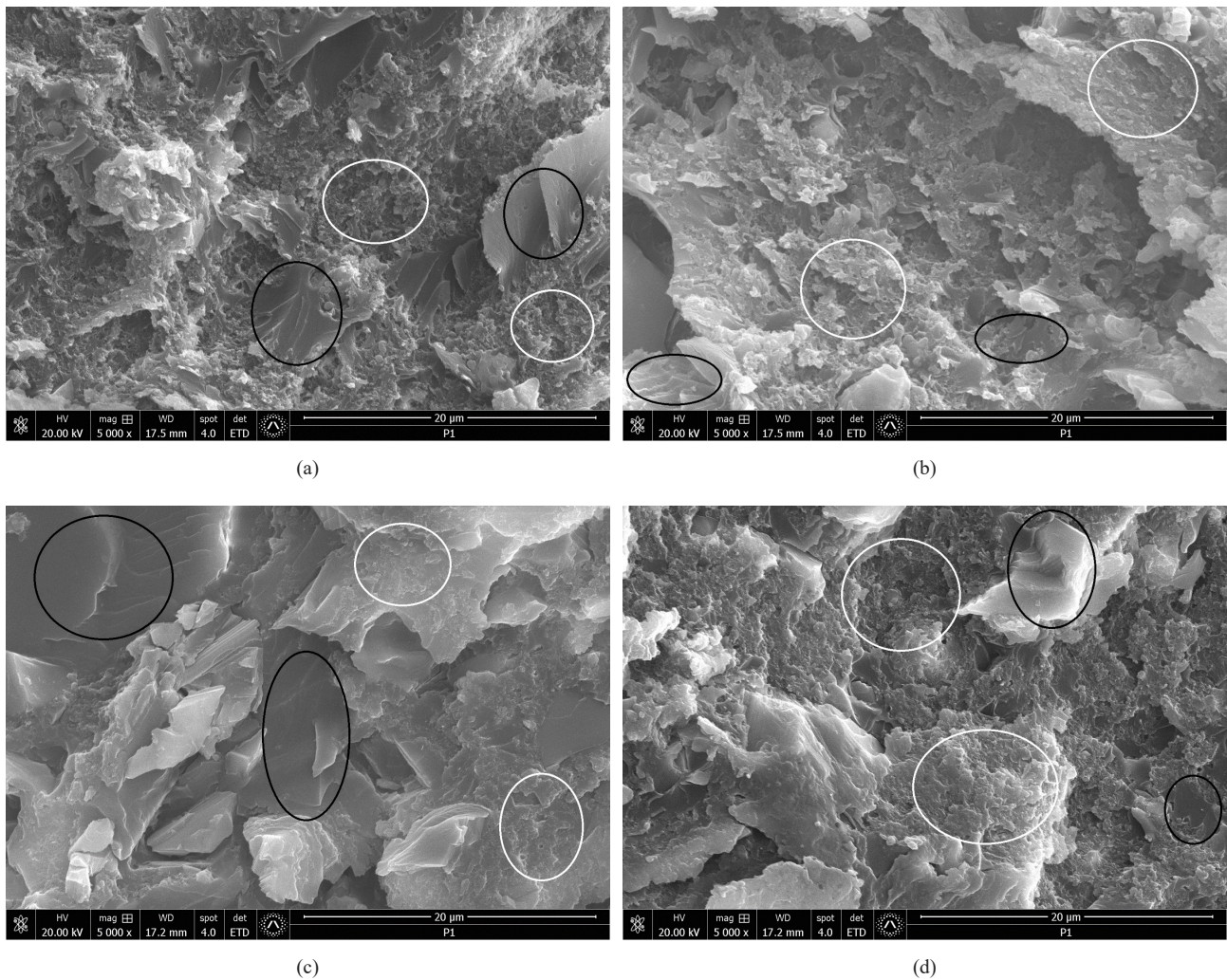
Figure 4. Microscopic failure mode as a function of CNT concentration: (a) 0.0 wt% CNT; (b) 0.25 wt% CNT; (c) 0.50 wt% CNT; (d) 1.00 wt% CNT
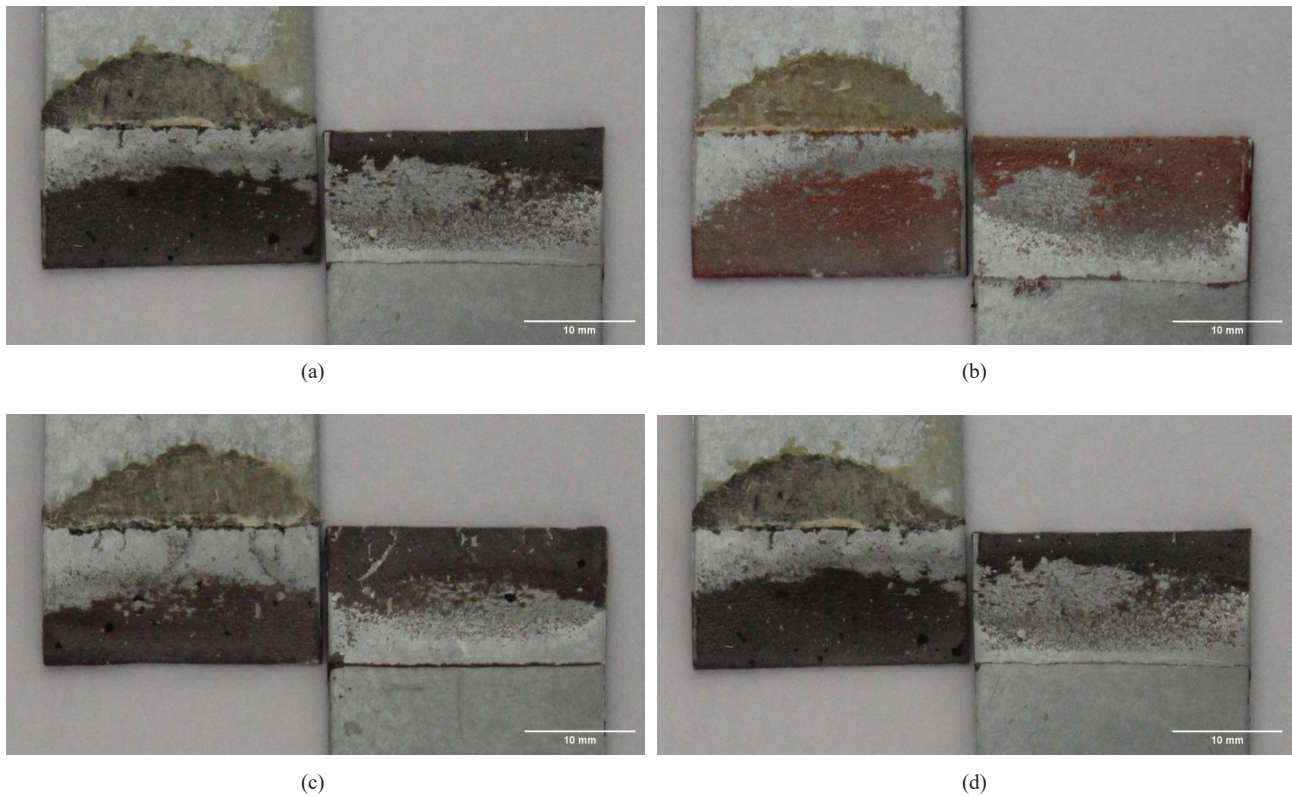
A mix of ductile-like/brittle-like behavior was observed in the baseline samples (0 wt% CNT), see Figure 4(a). This hypothesis can be verified by the two different fracture patterns observed. The first one is defined by cleavage and smooth fractures, typical of a brittle-like morphology (dark circles), while the "ductile-like" phase is mainly described by small fracture areas (white circles). For the micrograph's clearness, only two samples of each fracture type are marked with circles (black or white). The Carbon Nanotube (CNT) addition also affected the overall failure morphology. For the CNT concentration of 0.25 wt%, the fracture morphology is similar to the one without CNT. However, the ratio between fracture modes areas (brittle-like/ductile-like) is different. The ratio changed from 0.28 for the baseline group (P-0.00) to 0.64 for the 0.25 wt% CNT content group (P-0.25). These changes can be explained by a competing mechanism, the first phenomenon is the increase in mechanical properties (apparent shear strength and strain at failure) by the CNT addition. The second mechanism is defined as changes in chemical functional intensity at the molecular level due to interactions among chemical functionals and CNTs. The first hypothesis was verified by Razavi et al. [35], who experimentally detected an increase in both apparent shear strength and elongation with the addition of nanoparticles, in their case nanoclay and carbon nanotubes. Moreover, as can see in Figures 4(b-c), the amount of CNTs influenced morphology formation. The dispersion of 0.50 wt% CNT concentration into the epoxy system had a double effect, i.e., the increase in the load-bearing and changes in fracture morphology. The brittle-like fracture mode is prevalent in this case (brittle/ductile ratio equals 2.34). A further increase in the CNT concentration produced an additional growth of load bearing. According to Monteiro and Ávila [6], this phenomenon was expected as the 1.0 wt% CNT content is below the saturation limit. The failure morphology was changed from brittle-like (0.5 wt% CNT) to a mixed mode, where the brittle-like/ductile-like ratio was around 0.32.

To understand why the failure morphologies changed from case to case, an FTIR analysis was performed. Before analyzing data obtained some comments must be made. A similar investigation was performed by Ejaz et al. [30]. As stated by Ejaz et al. [30], "similar spectra were observed for MWCNT, $MWCT_{COOH}$, and $MWCNT_{NH2}$ enhanced adhesive combinations in comparison to the net adhesive, and no new peak(s) was/were observed" (last paragraph of section 3.2, page 7). By observing Ejaz's observations, it is possible to conclude that net resin is controlling the "key" chemical functionals. The chemical bonds created between CNT or MWCNT, as called by Ejaz's research group, and the adhesive can be translated by changes in intensities in these "key" chemical functionals, as no new peaks were detected with the CNT addition. Figure 3(b) shows the FTIR signatures for each group investigated. Moreover, Table 2 shows the absorbance intensity ratio between each group with CNT addition and the baseline group. By analyzing Figure 3(b) and Table 2, it is clear that the same pattern as described by Ejaz et al. [30] was observed, therefore, it is possible to conclude that an enhancement in adhesive combination was reached.

Table 2. FTIR absorbance selected data aspect ratio of samples

Wavenumber [cm⁻¹]	$A_{0.25}/A_{0.00}$ [a.u]	$A_{0.50}/A_{0.00}$ [a.u]	$A_{1.00}/A_{0.00}$ [a.u]
695	0.89	0.40	1.07
756	0.91	0.38	1.06
836	1.00	0.33	0.94
1,176	0.97	0.35	0.95
1,247	0.86	0.16	1.68
1,514	0.98	0.23	0.90
1,593	0.91	0.27	1.10
2,967	0.91	0.30	0.86
3,330	0.91	0.33	0.88

Figure 5. Macroscopic failure modes as a function of CNT concentration: (a) 0.0 wt% CNT; (b) 0.25 wt% CNT; (c) 0.50 wt% CNT; (d) 1.00 wt% CNT

As discussed by Ramirez-Herrera et al. [36], small absorbance values can be translated as a small number of bonds at each specific wavenumber. Moreover, the wavenumber band between 756-572 cm^{-1} represents a typical rotation of the CH$_2$ functional group, while the stretching of C-O-C oxirane groups is denoted by the 836 cm^{-1} group. The 1,176 cm^{-1} peak denotes the C-O stretching of the aromatic ring, while the 1,247 cm^{-1} peak is an indication of the C-O-C functional group of ethers was stretched. The aromatic ring C-C stretching can be detected for epoxy systems at 1,514 cm^{-1} wavelength, while the aromatic ring C = C chemical bound stretching was identified at 1,593 cm^{-1}. The peak at 2,967 cm^{-1} wavenumber is an indication of an asymmetrical vibration CH$_2$. Moreover, O-H stretching vibrations can be recognized at the 3,330 cm^{-1} wavenumbers. By observing each fracture morphology and the correspondent FTIR some conclusions can be drawn. The ductile-like fracture is controlled by changes in the aromatic ring (C-O stretching at 1,176 cm^{-1}, C-C stretching at 1,514 cm^{-1}, and C = C stretching at 1,593 cm^{-1}) and ethers group (C-O-C stretching at 1,247 cm^{-1}). Changes in the ethers group have less influence than the ones in aromatic rings. (see Table 2). A small change in intensity means, such as observed in 1,247 cm^{-1} wavelength, smaller interaction between CNTs, and the adhesive chemical functionals. Therefore, they are "less effective" in the overall mechanical response. This hypothesis can be demonstrated by the increase in absorbance ratio at this wavelength for the 1.0 wt% CNT content. However, the brittle/ductile area ratio (0.32) is similar to the baseline system (0.28). The brittle/ductile area ratio distinct values can also be credited to adjustments to the oxirane groups (C-O-C stretching at 836 cm^{-1}, and rotations of CH$_2$ at 695 and 756 cm^{-1}). A small increase in absorbance ratio at these wavelengths for the 1.0 wt% CNT content was observed. Therefore, the morphological changes in brittle-like failure modes can be controlled by these chemical functional changes. Notice that for 0.50 wt% CNT content, the number of bonds is small. This hypothesis can be confirmed by the decrease in intensity at the entire spectrum from 4,000 cm^{-1} to 400 cm^{-1}. Notice that all A$_{0.50}$/A$_{0.00}$ aspect ratios are less than unity. A small number of chemical bonds are linked to premature/brittle-like failure. However, another mechanism is acting simultaneously, the carbon nanotube capability of "changing" the crack propagation path. This phenomenon can be observed in Figure 2(c) where brittle-like fractures have different propagation directions. According to Cameselle-

Molares et al. [37], the crack propagation is always perpendicular to the principal stress (σ_1). Therefore, different fracture propagations can only be explained by the carbon nanotube addition to the adhesive.

The final analysis is regarding the macroscopic failure analysis and the numerical model. By observing Figures 5(a-d), it is possible to conclude that in all cases the mix mode, i.e., cohesive/adhesive, failure is present. Moreover, the aspect ratio between the two failure areas is similar for all, but the 0.50 wt% CNT content. The cohesive/adhesive ratios are 66/34, 65/35, 55/45, and 67/33 for 0.0, 0.25, 0.50, and 1.0 wt% carbon nanotube content, respectively. As the surface treatment is the same, for more details see Reis et al. [26], the differences can only be explained by the morphological changes generated by chemical functional variations. By analyzing the data shown previously, it is possible to conclude that ductile-like failure at a microscopic level is related to macroscopic cohesive failure mode. The sharp decrease in cohesive failure mode for the 0.50 wt% CNT content samples is related to the increase in brittle-like fracture formations. In order to establish a quantitative correlation between the apparent shear strength and failure modes, multivariable linear regression was conducted. This analysis yielded a linear correlation involving apparent shear strength, the aspect ratio of cohesive/adhesive, and ductile/brittle areas. The resulting findings are presented in Table 3.

Table 3. Mathematical model parameters

$$\tau_{app} = \beta_0 + \gamma\beta_1 + \delta\beta_2$$

$$\tau_{app} = apparent\ shear\ strength$$

$$\gamma = micromechanical\ variable = ratio\ \frac{brittle}{ductile}\ areas$$

$$\delta = macromechanical\ variable = ratio\ \frac{cohesive}{adhesive}\ areas$$

Regression Statistics			
Multiple R	R Square	Adjusted R Square	Standard error
0.994190842	0.98841543	0.96524629	0.159892769
Coefficient β_0	Coefficient β_1		Coefficient β_2
-25.28927559	7.267405451		18.57788657

4. Conclusions

Three major conclusions can be established: The first one is the link between the chemical changes triggered by the carbon nanotubes addition to an epoxy adhesive and the failure morphology was established. For this industrial adhesive, the ductile-like fracture is measured by changes in the aromatic ring and ether groups. The oxirane groups are related to the brittle-like microscopic failure. The second one is the correlations between the macroscopic failure modes and the chemical functionals. The cohesive failure is controlled by the ductile-like failure at the microscopic level, while the adhesive failure is related to the brittle-like failure. Based on FTIR signature the brittle-like failure is related to chemical changes at 695 cm^{-1} and 756 cm^{-1} wavelengths. Moreover, the ductile-like failure is controlled by changes in chemical functionals at 1,176 cm^{-1}, 1,247 cm^{-1}, and 1,514 cm^{-1} wavelengths. Lastly, from the obtained results a linear mathematical correlation between two distinct conditions, namely macroscopic quantities such as apparent shear strength and failure modes, and microscopic quantities such as ratios of brittle and ductile areas was established.

Acknowledgments

Conflict of interest

The authors declare that they have no known competing financial interests or personal relationships that could have appeared to influence the work reported in this paper.

References

[1] B. Ravishankar, S. K. Nayak, and M. A. Kader, "Hybrid composites for automotive applications-A review," *Journal of Reinforced Plastics and Composites*, vol. 38, no. 18, pp. 835-845, 2019.

[2] A. C. Marques, J. A. Fuinhas, and C. Tomás, "Energy efficiency and sustainable growth in industrial sectors in European Union countries: A nonlinear ARDL approach," *Journal of Cleaner Production*, vol. 239, 2019.

[3] I. A. Tajudeen, A. Wossink, and P. Banerjee, "How significant is energy efficiency to mitigate CO_2 emissions? Evidence from OECD countries," *Energy Economics*, vol. 72, pp. 200-221, 2018.

[4] W. He, Y. Yang, Z. Wang, and J. Zhu, "Estimation and allocation of cost savings from collaborative CO_2 abatement in China," *Energy Economics*, vol. 72, pp. 62-74, 2018.

[5] X. Li, Z. Tan, L. Wang, J. Zhang, Z. Xiao, and H. Luo, "Experimental investigations of bolted, adhesively bonded and hybrid bolted/bonded single-lap joints in composite laminates," *Materials Today Communications*, vol. 24, pp. 101244, 2020.

[6] E. C. Monteiro and A. F. Ávila, "Improving single-lap joint load bearing by bioinspired interlocking patterns on substrates," *International Journal of Adhesiion and Adhesives*, vol. 113, pp. 103043, 2022.

[7] K. Matsumoto, T. Ishikawa, and T. Tanaka, "A novel joining method by using carbon nanotube-based thermoplastic film for injection over-molding process," *Journal of Reinforced Plastics and Composites*, vol. 38, no. 13, pp. 616-627, 2019.

[8] S. Mohammadi, M. Yousefi, and M. Khazaei, "A review on composite patch repairs and the most important parameters affecting its efficiency and durability," *Journal of Reinforced Plastics and Composites*, vol. 40, no. 1-2, pp. 3-15, 2021.

[9] A. F. Ávila and K. K. Tamma, "Analysis of laminate metal matrix composites," *Journal of Thermal Stresses*, vol. 21, no. 9, pp. 897-917, 1998.

[10] A. F. Avila and K. K. Tamma, "An integrated micro/macro modeling and computational methodology for high temperature composites," in *Thermal Stress V*, 1st ed., R. B. Hetnarski, Ed. Rochester: Lastran Publishing House, 1999, pp. 145-256.

[11] G. Carley, V. Geraldo, S. De Oliveira, and A. F. Avila, "Nano-engineered composites: Interlayer carbon nanotubes effect," *Materials Research*, vol. 16, no. 3, pp. 628-634, 2013.

[12] Z. Feng, M. Wang, R. Lu, W. Xu, T. Zhang, T. Wei, J. Zhang, and Y. Liao, "A composite structural high-temperature-resistant adhesive based on in-situ grown mullite whiskers," *Materials Today Communications*, vol. 23, pp. 100944, 2020.

[13] X. Shang, E. A. S. Marques, J. J. M. Machado, R. J. C. Carbas, D. Jiang, and L. F. M. da Silva, "Review on techniques to improve the strength of adhesive joints with composite adherends," *Composites Part B: Engineering*, vol. 177, pp. 107363, 2019.

[14] M. D. Banea and L. F. M. M. Da Silva, "Adhesively bonded joints in composite materials: An overview," *Proceedings of the Institution of Mechanical Engineers Part L: Journal of Materials: Designs and Applications*, vol. 223, no. 1, pp. 1-18, 2009.

[15] T. Zhang, J. Meng, Q. Pan, and B. Sun, "The influence of adhesive porosity on composite joints," *Composites Communications*, vol. 15, pp. 87-91, 2019.

[16] A. F. Ávila and D. T. S. Morais, "Modeling nanoclay effects into laminates failure strength and porosity," *Composite Structures*, vol. 87, no. 1, pp. 55-62, 2009.

[17] K. Yildiz, İ. Gürkan, F. Turgut, F. Cebeci, and H. Cebeci, "Fracture toughness enhancement of fuzzy CNT-glass fiber reinforced composites with a combined reinforcing strategy," *Composites Communications*, vol. 21, 2020.

[18] E. C. Monteiro and A. F. Avila, "The carbon nanotubes effect into single-lap joint failure modes and load capacity: A macromechanical analysis," *Materials Research*, vol. 20, pp. 143-152, 2017.

[19] H. N. P. Oliva and A. F. Avila, "Bonded joints with 'nano-stitches': Effect of carbon nanotubes on load capacity and failure modes," *Latin American Journal of Solids and Structures*, vol. 14, no. 4, pp. 674-684, 2017.

[20] S. G. Leão, M. G. de Melo Martins, N. C. F. Menezes, F. L. R. de Mendonça Lima, C. F. Silva, G. C. Arantes, and A. F. Ávila, "Experimental multi-scale analysis of carbon/epoxy composites nano-reinforced by carbon nanotubes/ multi-layer graphene," *Materials Research*, vol. 20, pp. 134-142, 2017.

[21] A. F. Ávila, L. V. Donadon, and H. V. Duarte, "Modal analysis on nanoclay epoxy-based fiber-glass laminates," *Composite Structures*, vol. 83, no. 3, pp. 324-333, 2008.

[22] H. V. Duarte, L. V. Donadon, and A. F. Ávila, "Mechanical properties of nanocomposite laminated structure and its sensibility to modal analysis procedure," *Latin American Journal of Solids and Structures*, vol. 11, no. 2, pp. 245-259, 2014.

[23] R. C. Santiago, R. L. Azevedo, A. F. Avila, and M. Alves, "Mechanical characterization of glass/epoxy composite material with nanoclays," In Proceeding of the 19th International Congress of Mechanical Engineering-COBEM, 2007, vol. 19, pp. 1-8.

[24] A. F Avila, M. I. Soares, and A. S. Neto, "An experimental investigation on nanocomposites under impact loading," *WIT Transation Engineering*, vol. 49, no. 1. pp. 89-101, 2005.

[25] A. F. Ávila, E. C. Dias, D. T. L. D. Cruz, M. I. Yoshida, A. Q. Bracarense, M. G. R. Carvalho, and J. D. Ávila Junior, "An investigation on graphene and nanoclay effects on hybrid nanocomposites post fire dynamic behavior," *Materials Research*, vol. 13, no. 2, pp. 143-150, 2010.

[26] M. O. dos Reis, H. Nascimento, E. C. Monteiro, S. G. Leão, and A. F. Ávila, "Investigation of effects of extreme environment conditions on multiwall carbon nanotube-epoxy adhesive and adhesive joints," *Polymer Composites*, vol. 43, no. 10, pp. 7500-7513, 2022.

[27] H. Nascimento, M. O. dos Reis, E. C. Monteiro, and A. F. Ávila, "An investigation on industrial adhesive nano-modified by graphene nanoplatelets under extreme environmental conditions," *International Journal of Adhesion and Adhesives*, vol. 111, 2021.

[28] H. Ejaz, A. Mubashar, E. Uddin, and Z. Ali, "A comparative study of GNPs and MWCNTs additives on dispersion behavior and strength characteristics of the adhesively bonded joints," *Journal of Dispersion Science and Technology*, pp. 1-12, 2022.

[29] ASTM International, "Standard test method for apparent shear strength of single-lap-joint adhesively bonded metal specimens by tension loading (Metal-to-Metal)," *ASTM International*, vol. 1, no. 74302, pp. 10-15, 2010.

[30] H. Ejaz, A. Mubashar, E. Uddin, Z. Ali, and N. Arif, "Influence of MWCNTs on strength properties of high viscous epoxy adhesive and fracture behavior of adhesively bonded joints," *Theoratical and Applied Fracture Mechanics*, vol. 120, pp. 103412, 2022.

[31] M. O. Dos Reis, L. de Paula, S. G. Leão, T. O. T. Ximenes, E. C. Monteiro, and A. F. Ávila, "A piece-wise hybrid fatigue approach applied to ageing: The single-lap composite joints case study," *2022 AIAA SciTech Forum and Exposition*, pp. 1-12, 2022.

[32] Q. G. Zeng and C. T. Sun, "Novel design of a bonded lap joint," *AIAA Journal*, vol. 39, no. 10, pp. 1991-1996, 2001.

[33] M. Naderi and F. Ebrahimi, "Fracture surface and mechanical properties of epoxy composites," *Epoxy Composites: Fabrication, Charicatorization and Applications*, pp. 259-298, 2021.

[34] A. H. Korayem, M. R. Barati, G. P. Simon, X. L. Zhao, and W. H. Duan, "Reinforcing brittle and ductile epoxy matrices using carbon nanotubes masterbatch," *Composites Part A: Applied Science and Manufacturing*, vol. 61, pp. 126-133, 2014.

[35] S. M. J. Razavi, M. R. Ayatollahi, A. Nemati Giv, and H. Khoramishad, "Single lap joints bonded with structural adhesives reinforced with a mixture of silica nanoparticles and multi walled carbon nanotubes," *International Journal of Adhesion and Adhesives*, vol. 80, pp. 76-86, 2018.

[36] C. A. Ramírez-Herrera, I. Cruz-Cruz, I. H. Jiménez-Cedeño, O. Martínez-Romero, and A. Elías-Zúñiga, "Influence of the epoxy resin process parameters on the mechanical properties of produced bidirectional [± 45°] carbon/epoxy woven composites," *Polymers*, vol. 13, no. 8, 2021.

[37] A. Cameselle-Molares, R. Sarfaraz, M. Shahverdi, T. Keller, and A. P. Vassilopoulos, "Fracture mechanics-based progressive damage modelling of adhesively bonded fibre-reinforced polymer joints," *Fatigue and Fracture of Engineering Materials & Structres*, vol. 40, no. 12, pp. 2183-2193, 2017.